Transmission Phase in the Kondo Regime Revealed in a Two-Path Interferometer

S. Takada,[1,*] C. Bäuerle,[2,3] M. Yamamoto,[1,4] K. Watanabe,[1] S. Hermelin,[2,3] T. Meunier,[2,3] A. Alex,[5] A. Weichselbaum,[5] J. von Delft,[5] A. Ludwig,[6] A. D. Wieck,[6] and S. Tarucha[1,7,†]

[1]*Department of Applied Physics, University of Tokyo, Bunkyo-ku, Tokyo 113-8656, Japan*
[2]*Université Grenoble Alpes, Institut NEEL, F-38042 Grenoble, France*
[3]*CNRS, Institut NEEL, F-38042 Grenoble, France*
[4]*PRESTO, JST, Kawaguchi-shi, Saitama 331-0012, Japan*
[5]*Physics Department, Arnold Sommerfeld Center for Theoretical Physics, and Center for NanoScience, Ludwig-Maximilians-Universität, Theresienstraße 37, 80333 München, Germany*
[6]*Lehrstuhl für Angewandte Festkörperphysik, Ruhr-Universität Bochum, Universitätsstraße 150, 44780 Bochum, Germany*
[7]*RIKEN Center for Emergent Matter Science (CEMS), 2-1 Hirosawa, Wako-shi, Saitama 31-0198, Japan*

(Received 21 November 2013; published 15 September 2014)

We report on the direct observation of the transmission phase shift through a Kondo correlated quantum dot by employing a new type of two-path interferometer. We observed a clear $\pi/2$-phase shift, which persists up to the Kondo temperature T_K. Above this temperature, the phase shifts by more than $\pi/2$ at each Coulomb peak, approaching the behavior observed for the standard Coulomb blockade regime. These observations are in remarkable agreement with two-level numerical renormalization group calculations. The unique combination of experimental and theoretical results presented here fully elucidates the phase evolution in the Kondo regime.

DOI: 10.1103/PhysRevLett.113.126601 PACS numbers: 72.10.Fk, 72.20.Dp, 73.23.Hk, 85.35.Ds

The Kondo effect, an archetype of many-body correlations, arises from the interaction between a localized spin and surrounding conduction electrons [1]. It is characterized by a many-body singlet ground state, often referred to as the Kondo cloud. It was first observed in metals with a small inclusion of magnetic impurities and manifests itself by a logarithmic increase of the electrical resistance at low temperatures. Recently, the advance in nanotechnology has made it possible to study the interaction of a single impurity spin in contact with an electron reservoir, in particular in semiconductor quantum dots (QDs) [2,3]. These developments have also allowed access to the phase shift across a Kondo impurity, a central ingredient of Nozières' celebrated Fermi-liquid theory for the low-energy fixed point of the Kondo effect [4]: when an electron of sufficiently low energy is incident on the impurity in the screened singlet state, it scatters coherently off the latter, acquiring a $\pi/2$-phase shift, but with zero probability for a spin flip. This $\pi/2$-phase shift is one of the hallmarks of the Kondo effect. Though it cannot be measured directly in conventional Kondo systems, it has been suggested [5] to be possible for a semiconductor QD placed in one arm of an Aharonov-Bohm (AB) ring, where the transmission phase through the dot can be extracted from the AB oscillations of the conductance as a function of the magnetic flux through the ring [6,7]. For such geometries it has been predicted that the $\pi/2$-phase shift should persist, perhaps surprisingly, even up to temperatures as high as the Kondo temperature, T_K [8,9].

Such Kondo phase measurements have indeed been pursued in a number of remarkable pioneering experiments [10–14]. However, unexpected results have been obtained for the phase shift in the Kondo regime ($T \lesssim T_K$): for instance, Ref. [10] reported a π plateau in the Kondo valley and the total phase change through the spin-degenerate pair was of about 1.5π, while Ref. [11] reported an almost linear phase shift over a range of 1.5π when the Fermi energy was scanned through a spin degenerate level. Explanations of these surprising features are still lacking. The $\pi/2$ plateau in the Kondo valley has only been reported in Ref. [12]. In that measurement, however, the temperature was so large ($T/T_K \gtrsim 30$) that Kondo correlations are strongly suppressed. In such conditions one does not expect to observe the $\pi/2$-Kondo phase shift, which is predicted to occur only for $T < T_K$ [5]. Another puzzling feature of this experiment is that the $\pi/2$-phase shift extends over the entire Kondo valley. According to Kondo theory [5,9], one would actually expect a strong phase dependence within the Kondo valley for the experimental conditions of Ref. [12] (see Ref. [15]).

In this Letter, we report on measurements of the transmission phase shift through a Kondo QD using an original two-path interferometer. We confirm the π-phase shift across a Coulomb peak (CP) without Kondo correlation as expected from a Breit-Wigner type resonance. In the Kondo regime, we observe a clear $\pi/2$-phase shift at $T \lesssim T_K$. Increasing T above T_K, the phase shift starts to deviate from the $\pi/2$ behavior and approaches the one observed for the standard Coulomb blockade regime. Via complementary two-level numerical renormalization group calculations [9,18–21] we obtain a detailed and consistent understanding of the phase behavior in the Kondo regime.

The measurement of the true transmission phase through a QD in an AB setup is not at all trivial. Multiple path contributions by electrons that encircle the AB loop multiple times alter the phase of the observed AB oscillation and a reliable extraction of the *true* transmission phase through a QD is impossible. The most conspicuous example is the so-called phase rigidity [22,23] in a two-terminal setup. It has been shown that employing multi-terminal devices can lift the phase rigidity [7,10–12,24]. However, it is far from obvious that in such a device multiple path contributions are sufficiently suppressed. In contrast, with our original two-path interferometer we are able to suppress such multiple path contributions.

The device was fabricated in a two-dimensional electron gas [2DEG, $n = 3.21 \times 10^{11}$ cm^{-2}, $\mu = 8.6 \times 10^5$ cm^2/V s at 4.2 K; see Fig. 1(a)] formed at an AlGaAs/GaAs heterointerface with standard surface Schottky gate technique. It consists of a novel AB interferometer, where the AB ring is attached to two tunnel-coupled wires, and acts as a *true* two-path interferometer when the tunnel-coupled wires are set to work as half beam splitters by carefully tuning the tunnel gate voltages V_{T1} and V_{T2} [25]. This does not degrade the current oscillation signal (maximum visibility ~15%) in contrast with multiterminal devices employed in previous works, where most of the coherent electrons are lost in the base contacts. The unique advantage of this device is that the true transmission phase can be determined with very high accuracy since contributions from the multipath interferences can be fully eliminated by simply tuning the gate voltages such that the two output currents I_1 and I_2 oscillate with opposite phase as a function of the magnetic field [25]. In this case, the total current $(I_1 + I_2)$ through the interferometer shows no magnetic field dependence, a signature that loop trajectories are suppressed, leaving only the two-path interference. The phase extracted from the antiphase oscillations of I_1 and I_2 is always reproducible and consistent with theoretical expectations. In contrast, when I_1 and I_2 are not antiphase due to the existence of multiple loops, the phase of the current oscillation becomes different from the reproducible and consistent one even if it smoothly shifts with the voltages on one of the gates forming the AB ring, suggesting the possibility that previous experiments [10–12] might still have suffered from multiple path contributions [26–29]. All the measurements were done in a dilution refrigerator at a base temperature of approximately 15 mK, except for Fig. 2(a) and Fig. 3(c). For the transport measurements an ac bias ($3 \sim 20$ μV, $f = 23.3$ Hz) was applied to the lower left contact and currents I_1 and I_2 were measured at the two output contacts using a standard lock-in technique. This bias is sufficiently small that the current response is linear to deduce the differential conductance of the system studied here.

To characterize the sample, we first measured the transmission phase shift across a CP without Kondo correlation, where the temperature is much larger than T_K. Transport only through the QD was achieved by depleting the left tunnel gate V_{T1}; Fig. 1(b) shows the corresponding current I_2^*. For the phase measurement, the left tunnel-coupled wire was then tuned to a half beam splitter. For each value of V_p the magnetic field dependencies of the two output currents I_1 and I_2 are recorded. In order to extract the oscillating part, we subtract the smoothed background from the raw data [31] (see Ref. [15]). The dependence of the transmission phase shift

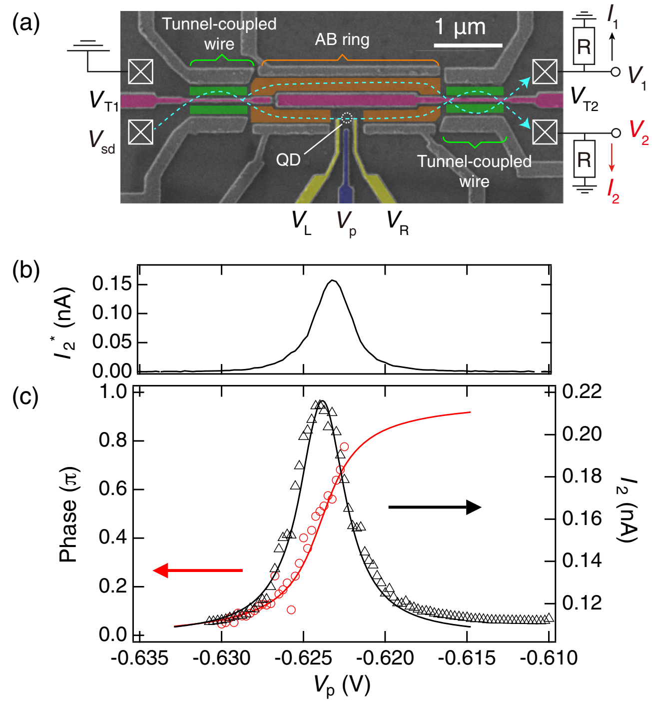

FIG. 1 (color online). (a) Scanning electron micrograph of the employed device and measurement setup. The AB ring is connected to a tunnel-coupled wire on both sides. A QD is embedded into the lower path of the AB ring. The dashed lines indicate the two paths. The current flowing through the upper (lower) contact is obtained from $I_{1(2)} = V_{1(2)}/R$ ($R = 10$ kΩ). (b) Coulomb peak of the QD in the Coulomb blockade regime, where I_2^* corresponds to the current passing only through the QD by completely depleting the left tunnel gate V_{T1}. The energy level of the QD is scanned across the Fermi energy by changing the plunger gate voltage V_p. A charging energy $U \sim 1.8$ meV, a tunnel-coupling energy $\Gamma \sim 40$ μeV, and a single level spacing $\delta \sim 230$ μeV were estimated by mapping out the Coulomb diamond (not shown here). (c) Phase evolution across the Coulomb peak extracted from the antiphase oscillations is plotted on the left axis (red circles). The current collected in I_2 is plotted on the right axis (black triangles), where I_2 is averaged over one oscillation period of magnetic field. For gate voltages more positive than -0.623 V, charging noise did not allow us to follow the oscillations and reliable data of the transmission phase could not be obtained. Black and red solid lines show Lorentzian fitting of I_2 and the transmission phase expected from Friedel's sum rule (see text), respectively.

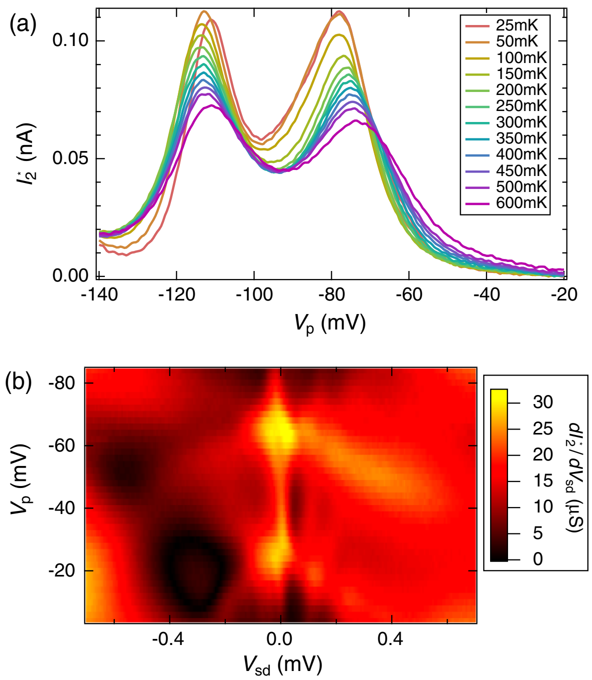

FIG. 2 (color online). (a) Temperature dependence of two Coulomb peaks which show Kondo correlations, observed in I_2^* plotted as a function of V_p, where the left tunnel gate V_{T1} was depleted. Here $V_{sd} \sim 3.5\ \mu$V was applied to measure the current. (b) Coulomb diamond for the CPs shown in (a) in the Kondo regime ($T \lesssim T_K$). The gate voltage configuration in (b) differs from that in (a) by a V_p shift of ~50 mV, because (b) was measured using slightly wider one-dimensional channels for the leads, to get rid of some additional V_p independent structures in the Coulomb diamond coming from the narrow one-dimensional channels [30], which disappeared upon slightly widening the channels.

on V_p is then obtained by performing a complex fast Fourier transform (FFT) of the oscillating part [12,31,32]. Other gate voltages are fixed during the measurement.

The extracted phase is shown in Fig. 1(c). The shape of the current I_2 mimics that of the CP I_2^*, apart from an additional finite background current due to the current flowing through the upper path. Here we show the non-oscillating part of I_2 averaged over one oscillation period of the magnetic field. The change in the transmission phase $\Delta\varphi_{dot}$ with changing plunger gate voltage is related to the corresponding change in QD charge (in units of the electron charge) ΔN, via Friedel's sum rule, $\Delta N = \Delta\varphi_{dot}/\pi$ [33]. The red solid line in Fig. 1(c) shows the phase extracted from the averaged I_2 via Friedel's sum rule. First, I_2 is fitted by a Lorentzian function to obtain a continuous line shape of the CP (black solid line), which also gives the total area of the CP. ΔN as a function of V_p is then given by the integrated area under the fitted CP up to V_p divided by the total area of the CP. The measured phase shift shown by the red circles across the CP is in very good agreement with the phase extracted using Friedel's sum rule [33].

We then focused on a pair of CPs and tuned them into the Kondo regime by V_L, V_p, V_R [see Fig. 1(a)]. We first characterized the QD using transport measurements only through the dot. Panel (a) of Fig. 2 shows the temperature dependence of two CPs, where the Kondo effect appears in the valley between the two peaks around a plunger gate voltage of -100 mV. The current I_2^* in the valley increases as the temperature is lowered, a clear signature of the Kondo effect. As we do not reach the unitary limit, T_K cannot be determined with high precision from this temperature dependence of the conductance, but we find an upper bound of approximately 100 mK for the Kondo temperature at the valley center. Figure 2(b) shows a Coulomb diamond in this regime and a clear maximum (vertical yellow ridge) is observed around zero bias in the Coulomb blockade region, usually referred to as the zero bias anomaly.

The transmission phase across these two CPs was then measured by opening the left tunnel gate V_{T1}, and recording the AB oscillations for different plunger gate voltages V_p, as shown in Fig. 3(a). In this experiment, the energy scale of the magnetic field was lower than that of the temperature, so that spin was not resolved [34]; however, we see clear signatures of the Kondo effect. The visibility of our AB oscillations is sufficiently large to reveal, even in the raw data, a clear phase shift of approximately $\pi/2$ in the Kondo valley, as indicated by the dotted lines in Fig. 3(a). To reveal the phase shift across the CPs even more clearly, we performed a complex FFT as described above. The obtained transmission phase is presented in Fig. 3(b), together with I_2. A total phase shift of π when scanning through the two successive CPs is observed and a clear plateau appears at $\pi/2$ in the Kondo valley. This result contrasts with the phase shift across a CP without Kondo correlation. Although the conductance does not reach the unitary limit, the transmission phase shift in the Kondo valley already shows the $\pi/2$-phase shift, which is consistent with theoretical predictions that the $\pi/2$-phase shift survives for temperature as large as $T \sim T_K$ [8,9].

When increasing the temperature to approximately 110 mK, the Kondo correlations are reduced ($T \gtrsim T_K$) and the behavior of the transmission phase is slightly altered. The phase climbs slightly above $\pi/2$ before decreasing slightly, forming an S-shape [Fig. 3(c)] in the Kondo valley. To further reduce the Kondo correlations, we reduced the coupling energy Γ by suitably tuning V_L, V_p, V_R, which lowers the Kondo temperature [Fig. 3(d)], thus reaching a regime where $T \gg T_K$. In this regime, the S-shaped structure of the phase evolution is more pronounced and becomes asymmetric with respect to the valley center and the value $\varphi_{dot} = \pi/2$. This suggests that by further reducing the Kondo correlations the phase behavior across each CP would approach that observed for CPs without Kondo correlation. These results differ strikingly from the observation of Ref. [12], where a $\pi/2$-phase shift has been reported for a regime where $T \gg T_K$ (see Ref. [15]).

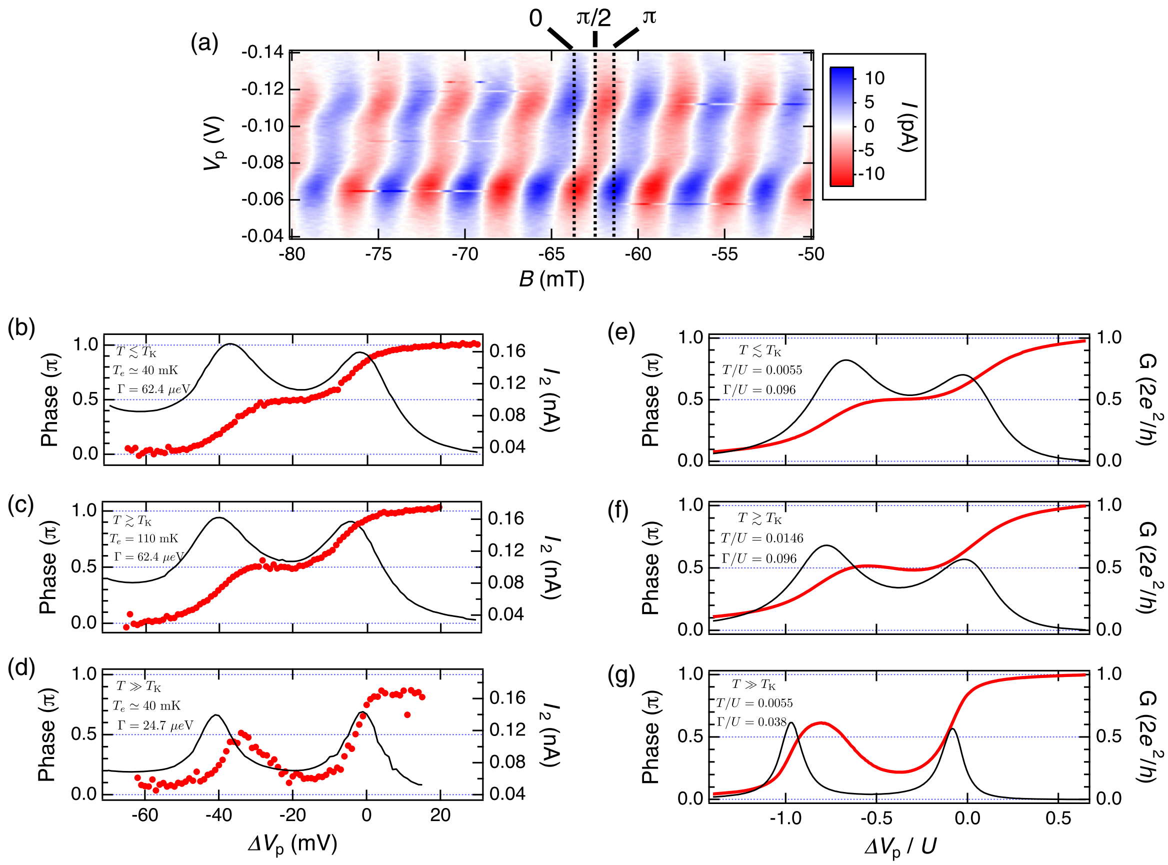

FIG. 3 (color online). (a) AB oscillation amplitude as a function of magnetic field, obtained for the same gate configurations as Fig. 2(a) except for V_{T1} by scanning the plunger gate voltage V_p across two successive Coulomb peaks, showing Kondo correlations in the valley between them ($T \lesssim T_K$). The AB oscillation amplitude is obtained from $I = I_1 - I_2$ by subtracting a smoothed background. Dotted lines emphasize the phase shift. (b),(c),(d) The transmission phase (red circles, left axis), determined by a complex FFT of the antiphase oscillations, together with I_2 (black line, right axis), plotted as a function of the change ΔV_p in plunger gate voltage with respect to its value at the center of the right CP, for three different regimes, (b): $T \lesssim T_K$, (c): $T \gtrsim T_K$, and (d): $T \gg T_K$. I_2 is averaged over one oscillation period of magnetic field. Parameters shown in the figures are estimates, extracted from fitting NRG results to the measured phase curves. (e),(f),(g) Transmission phase (red line) and conductance (black line) calculated by a two-level Anderson impurity model with $s = +$ and the lower level being the Kondo level, for an interaction energy $U = 650\ \mu$eV and a level spacing of $\delta = 0.5U$ (for details, see Ref. [15]). Fitting parameters used for the calculations are shown in the figures. Current I_2 of the experimental data (b),(c),(d) contains a linear background from the upper arm of the interferometer whereas the conductance G in the theoretical calculations (e),(f),(g) is the bare conductance across a QD.

To further corroborate our findings we performed numerical renormalization group (NRG) calculations of the conductance as well as of the transmission phase. We found that even when the single level spacing δ is larger than the coupling energy Γ, the contribution from multiple levels in the dot plays an important role for the phase behavior at $T \gg T_K$. Taking into account only a single level results in a phase evolution, which is symmetric with respect to the center of the Kondo valley, contrary to our experimental findings [see Fig. 3(d)]. In order to accurately reproduce the experimental phase data, we therefore employed a two-level Anderson model (see Ref. [15]). It is crucial to choose correctly the relative sign of the tunnel-coupling coefficients [i.e., $s = \mathrm{sgn}(t_L^1 t_R^1 t_L^2 t_R^2)$] for fitting the data of Fig. 3(d), since this sign characterizes the influence of the nearby orbital level on the phase evolution. Fitting the predicted phase evolution to the one observed experimentally (see Ref. [15]) allows us to estimate the QD parameters, such as Γ and δ, with good precision (note that these are not easily accessible only from the measured conductance data, due to renormalization of the CPs by the Kondo effect). In addition, the slope of the phase in the Kondo valley in Fig. 3(c) allows us to precisely evaluate the Kondo temperature at the valley center to $T_K \simeq 50$ mK for Figs. 3(b) and 3(c). From the temperature evolution of the $\pi/2$ plateau, which is most prominent close to T_K, we are able to evaluate the actual electron temperature to $T_e \sim 40$ mK, consistent with previous measurements in the same electromagnetic environment [35]. The most important finding, however, is the fact that the $\pi/2$-phase shift persists up to a temperature of T_K and then evolves into an S shape at higher temperatures, which is extremely well captured by the NRG calculations.

In summary, our measurements show that the transmission phase through a Kondo QD is $\pi/2$ up to temperatures of the order of T_K, in full agreement with theoretical expectations. The key new ingredient underlying this result is the use of a novel AB interferometer design that can be fine-tuned to reliably exclude the contributions of paths traversing the interferometer multiple times. This new design, in combination with detailed theoretical calculations for a two-level Anderson model, allowed us to obtain a detailed and consistent understanding of the behavior of the Kondo phase shift.

S. Takada acknowledges support from JSPS Research Fellowships for Young Scientists and French Government Scholarship for Scientific Disciplines. C. B. acknowledges financial support from the French National Agency (ANR) in the frame of its program BLANC FLYELEC Project No. anr-12BS10-001, as well as from DRECI-CNRS/JSPS (PRC 0677) International collaboration. M. Y. acknowledges financial support by Grant-in-Aid for Young Scientists A (No. 23684019) and Grant-in-Aid for Challenging Exploratory Research (No. 25610070). A. A., A. W., and J. v. D. acknowledge support from the DFR through SFB-631, SFB-TR12, and the Cluster of Excellence Nanosystems Initiative Munich, and from the Center for NanoScience. A. L. and A. D. W. acknowledge support from Mercur Pr-2013-0001, BMBF - Q.com-H 16KIS0109, and the DFH/UFA CDFA-05-06. S. Tarucha acknowledges financial support by JSPS, Grant-in-Aid for Scientific Research S (No. 26220710), MEXT KAKENHHI Quantum Cybernetics", MEXT project for Developing Innovation Systems, and JST Strategic International Cooperative Program.

*Present address: CNRS, Institut NEEL, F-38042 Grenoble, France.
†tarucha@ap.t.u-tokyo.ac.jp

[1] J. Kondo, Prog. Theor. Phys. **32**, 37 (1964).
[2] D. Goldhaber-Gordon, H. Shtrikman, D. Mahalu, D. Abusch-Magder, U. Meirav, and M. A. Kastner, Nature (London) **391**, 156 (1998).
[3] W. G. van der Wiel, S. De Franceschi, T. Fujisawa, J. M. Elzerman, S. Tarucha, and L. P. Kouwenhoven, Science **289**, 2105 (2000).
[4] P. Nozières, J. Low Temp. Phys. **17**, 31 (1974).
[5] U. Gerland, J. von Delft, T. A. Costi, and Y. Oreg, Phys. Rev. Lett. **84**, 3710 (2000).
[6] A. Yacoby, M. Heiblum, D. Mahalu, and H. Shtrikman, Phys. Rev. Lett. **74**, 4047 (1995).
[7] R. Schuster, E. Buks, M. Heiblum, D. Mahalu, V. Umansky, and H. Shtrikman, Nature (London) **385**, 417 (1997).
[8] P. G. Silvestrov and Y. Imry, Phys. Rev. Lett. **90**, 106602 (2003).
[9] T. Hecht, A. Weichselbaum, Y. Oreg, and J. von Delft, Phys. Rev. B **80**, 115330 (2009).
[10] Y. Ji, M. Heiblum, D. Sprinzak, D. Mahalu, and H. Shtrikman, Science **290**, 779 (2000).
[11] Y. Ji, M. Heiblum, and H. Shtrikman, Phys. Rev. Lett. **88**, 076601 (2002).
[12] M. Zaffalon, A. Bid, M. Heiblum, D. Mahalu, and V. Umansky, Phys. Rev. Lett. **100**, 226601 (2008).
[13] M. Sato, H. Aikawa, K. Kobayashi, S. Katsumoto, and Y. Iye, Phys. Rev. Lett. **95**, 066801 (2005).
[14] S. Katsumoto, H. Aikawa, M. Eto, and Y. Iye, Phys. Status Solidi (c) **3**, 4208 (2006).
[15] See Supplemental Material at http://link.aps.org/supplemental/10.1103/PhysRevLett.113.126601, which includes Refs. [16,17], for details of the working principle of the two-path interferometer, analysis of phase shift, NRG calculations, and comparison between present work and previous measurements of the transmission phase shift in the Kondo regime.
[16] Y. Meir and N. S. Wingreen, Phys. Rev. Lett. **68**, 2512 (1992).
[17] H.-W. Lee, Phys. Rev. Lett. **82**, 2358 (1999).
[18] K. G. Wilson, Rev. Mod. Phys. **47**, 773 (1975).
[19] A. Weichselbaum and J. von Delft, Phys. Rev. Lett. **99**, 076402 (2007).
[20] R. Bulla, T. A. Costi, and T. Pruschke, Rev. Mod. Phys. **80**, 395 (2008).
[21] A. Weichselbaum, Ann. Phys. (Amsterdam) **327**, 2972 (2012).
[22] M. Büttiker, IBM J. Res. Dev. **32**, 317 (1988).
[23] A. Yacoby, R. Schuster, and M. Heiblum, Phys. Rev. B **53**, 9583 (1996).
[24] M. Sigrist, A. Fuhrer, T. Ihn, K. Ensslin, S. E. Ulloa, W. Wegscheider, and M. Bichler, Phys. Rev. Lett. **93**, 066802 (2004).
[25] M. Yamamoto, S. Takada, C. Bäuerle, K. Watanabe, A. D. Wieck, and S. Tarucha, Nat. Nanotechnol. **7**, 247 (2012).
[26] O. Entin-Wohlman, A. Aharony, Y. Imry, Y. Levinson, and A. Schiller, Phys. Rev. Lett. **88**, 166801 (2002).
[27] A. Aharony and O. Entin-Wohlman, Phys. Rev. B **72**, 073311 (2005).
[28] P. Simon, O. Entin-Wohlman, and A. Aharony, Phys. Rev. B **72**, 245313 (2005).
[29] A. Aharony, O. Entin-Wohlman, Y. Oreg, and J. van Delft, Phys. Rev. Lett. **96**, 189705 (2006).
[30] A. Kristensen, H. Bruus, A. E. Hansen, J. B. Jensen, P. E. Lindelof, C. J. Marckmann, J. Nygård, C. B. Sørensen, F. Beuscher, A. Forchel, and M. Michel, Phys. Rev. B **62**, 10950 (2000).
[31] V. Chandrasekhar, R. A. Webb, M. J. Brady, M. B. Ketchen, W. J. Gallagher, and A. Kleinsasser, Phys. Rev. Lett. **67**, 3578 (1991).
[32] M. Avinun-Kalish, M. Heiblum, O. Zarchin, D. Mahalu, and V. Umansky, Nature (London) **436**, 529 (2005).
[33] A. Levy Yeyati and M. Büttiker, Phys. Rev. B **52**, R14360 (1995).
[34] A. Carmi, Y. Oreg, M. Berkooz, and D. Goldhaber-Gordon, Phys. Rev. B **86**, 115129 (2012).
[35] Y. Niimi, Y. Baines, T. Capron, D. Mailly, F.-Y. Lo, A. D. Wieck, T. Meunier, L. Saminadayar, and C. Bäuerle, Phys. Rev. B **81**, 245306 (2010).